

Theory of a Single-Atom Point Source for Electrons

N. D. Lang

IBM Research Division, Thomas J. Watson Research Center, Yorktown Heights, New York 10598

A. Yacoby and Y. Imry

Department of Nuclear Physics, Weizmann Institute of Science, Rehovot 76100, Israel

(Received 24 May 1989)

A theoretical analysis is presented of the current from a field-emission tip terminated by a single atom. The calculations yield a relatively focused, high-current beam with a narrow energy distribution, in agreement with recent experimental studies. The results are physically interpreted in terms of channel filtering by an adiabatic constriction.

PACS numbers: 79.70.+q, 41.80.Dd, 61.16.Di, 73.40.Gk

We analyze here the microscopic aspects of field emission from a tip on which the primary emission source is a single atom. The experimental background we consider is the work of Fink¹ on such "point sources" for electrons. Currents of a few microamps with fields of $\lesssim 1$ V/Å were obtained from well-characterized tips in these experiments, with emission into a very narrow beam.

Our model for this problem is one used earlier to study aspects of current flow in the scanning tunneling microscope:² two planar metallic electrodes with a bias between them, with an adsorbed atom kept fixed at its zero-field equilibrium distance on one of the electrodes. These two electrodes, one (with the atom) representing the tip and the other the screen, are separated in the calculation not by the distances of the order of centimeters typical in a field-emission experiment,³ but rather by a large but still atomic-scale distance (we use 30 bohrs). This, however, allows us to concentrate on the microscopic aspects of the problem of interest here, and largely avoid discussion of macroscopic effects in the experiment such as field focusing.

As in our earlier studies on the scanning tunneling microscope,² we will use the jellium model to represent the metallic electrodes themselves. Our solution proceeds as follows: First, within the framework of the density-functional formalism, we find the single-particle wave functions and self-consistent density distribution for the pair of bare metallic electrodes, assuming them, for simplicity, to be identical ($r_s = 2$ jellium model) in the presence of the bias voltage. This problem of the biased bimetallic junction has been discussed by McCann and Brown,⁴ and we follow in outline their procedure.

We next use the method of Lang and Williams⁵ to find the self-consistent density distribution and single-particle wave functions for the total system consisting of the two bare electrodes plus the atom. It will be recalled that this method was originally used to study an atom adsorbed on a single bare metallic surface, and proceeded by solving a Lippmann-Schwinger equation that involved a Green's function for the bare metal. The only significant difference here is that the Green's function is

that appropriate to the biased bimetallic junction, instead of the single surface. The wave functions are then used to obtain the current.

For bias V (defined here as positive), the current density at zero temperature is given by (using atomic units, with $|e| = \hbar = m = 1$)

$$\mathbf{j}(\mathbf{r}) = 2 \int_{\epsilon = -\infty}^{\epsilon = \epsilon_F^{\text{tip}}} d\mu \text{Im} \Psi_\mu^*(\mathbf{r}) \nabla \Psi_\mu(\mathbf{r}), \quad (1)$$

where Ψ_μ is a current-carrying state with quantum label μ , which in our case represents energy ϵ , azimuthal quantum number m , and parallel momentum label κ , and $\int d\mu$ is an integration over energy and a sum or integration over the other state labels as well. The upper limit of the energy integration is the tip-electrode Fermi level (ϵ_F^{tip}), and since the only states that make a significant contribution to the current are those not far in energy below ϵ_F^{tip} , we simply write the lower limit as $-\infty$. The factor of 2 is for spins, which we do not include in our label μ . The state Ψ_μ deep in the interior of the tip electrode consists of a plane wave moving toward the surface region plus reflected waves, and deep in the interior of the screen electrode consists only of transmitted waves.

We will be interested in the additional current density due to the presence of the atom, $\delta\mathbf{j}(\mathbf{r}) = \mathbf{j}(\mathbf{r}) - \mathbf{j}_0$, where \mathbf{j}_0 is the current density for the bimetallic junction in the absence of the atom, and in the total additional current δI , which can be obtained by integration of $\delta\mathbf{j}$ over an appropriate surface.

Now we will wish to plot a quantity such as δI against the induced electric field E (defined as positive) at the surface of our tip. By induced electric field we mean the difference in field between the cases with and without an applied bias. There will, in general, be a field in the vicinity of the tip atom, even in the absence of an applied bias, because under most circumstances such an atom, even if it is adsorbed on a cluster of the same type of atoms, will have a dipole moment. The "surface" of a one-atom tip is not well defined, and so we must choose the exact point in the vicinity of the atom at which to

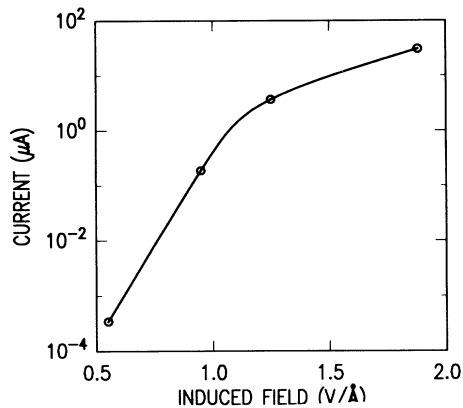


FIG. 1. Current δI vs induced electric field E with Na tip atom. Calculations were done for four field values (circles); these results are connected with a smooth curve.

evaluate E . This point will of course be chosen on the surface normal through the atomic nucleus. Now E as a function of distance along this line will have a maximum, since if we evaluate E at points close enough to the center of the atom that they lie inside of the charge cloud induced on the atom by the applied field, then only part of the cloud will contribute to E , while at points far outside this cloud, the value of E decreases as described by classical electrostatics.⁶ We will therefore evaluate E where it is a maximum.

Figure 1 shows the current δI as a function of induced electric field E . It is clear that for fields of the order of 1 V/Å, the current is of the order of that seen in the experiments of Fink.^{1,7} Figure 2 shows the (zero-temperature) total energy distribution curve $\delta I(\epsilon)$ for $E = 1.0$ V/Å; it is quite narrow, with a full width at half maximum of 120 meV.⁸

Figure 3 shows streamlines of $\delta j(\mathbf{r})$ for $E = 1.3$ V/Å. Streamlines in the immediate vicinity of the atom are not shown. The outermost ones define a surface containing half the current δI . The beam is seen to be fairly well focused, the main reason for which is discussed below. A subsidiary reason is that, in contrast to the usual experimental configuration, the screen is relatively close.⁹ That this is less important than the microscopic potential configuration within the dashed box, which will be similar to that in the experiment, is illustrated by the fact that a particular change in this configuration considered below (creation of a deep channel just to the right of the atom) is enough to cause the streamlines to spread out like a fan, with a maximum opening angle of over 70°.

Far from the region of the tip atom, the total effective potential $v_{\text{eff}}(\mathbf{r})$ (consisting of electrostatic plus exchange-correlation parts) seen by the field-emitted electrons is that of the bimetallic junction without the atom (Fig. 4); in the region near the atom—that enclosed by the dashed rectangle in Fig. 3— $v_{\text{eff}}(\mathbf{r})$ has the form shown in Fig. 5.

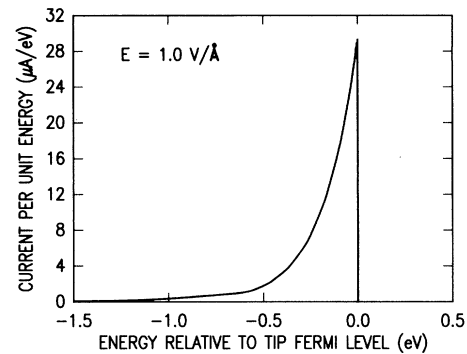


FIG. 2. Total energy distribution curve $\delta I(\epsilon)$ for $E = 1.0$ V/Å (zero temperature) with Na tip atom.

These maps give the contour $v_{\text{eff}}(\mathbf{r}) = \epsilon_F^{\text{tip}}$ (this is the solid one closest to the atom), as well as a number of other contours for values both above ϵ_F^{tip} and below ϵ_F^{tip} (dotted). Thus the areas filled with solid contours represent regions where an electron at the tip Fermi level encounters a potential barrier. (Recall from Fig. 2 that most of the current comes from states near the tip Fermi level.) At lower fields, the electron leaving the tip encounters a potential barrier in all directions toward the screen, but as the field is raised, a channel opens up through the solid-contour region, leading to a hornlike potential opening toward the screen.

The propagation of waves in adiabatic (slowly vary-

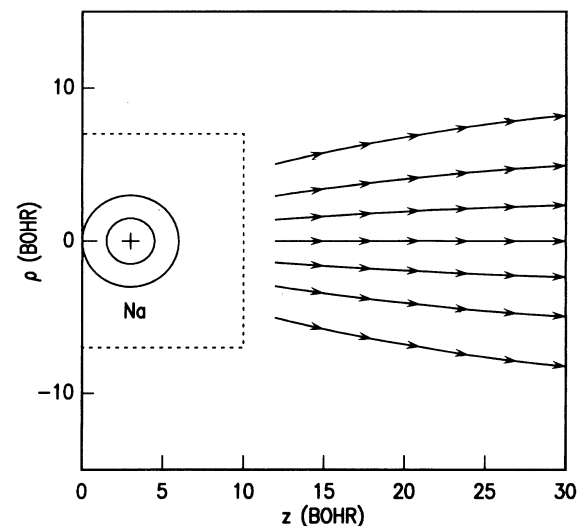


FIG. 3. Streamlines of $\delta j(\mathbf{r})$ for $E = 1.3$ V/Å and Na tip atom. Left and right edges of the box correspond to positive background edges of the two electrode surfaces. Coordinates ρ and z are parallel and perpendicular to the surfaces, respectively. The presence of the tip atom is indicated schematically by solid circles with the cross at the position of the nucleus. The outermost pair of streamlines encloses $\frac{1}{2} \delta I$. The potential v_{eff} within the region enclosed by the dashed rectangle is shown in Fig. 5 (1 bohr = 0.529 Å).

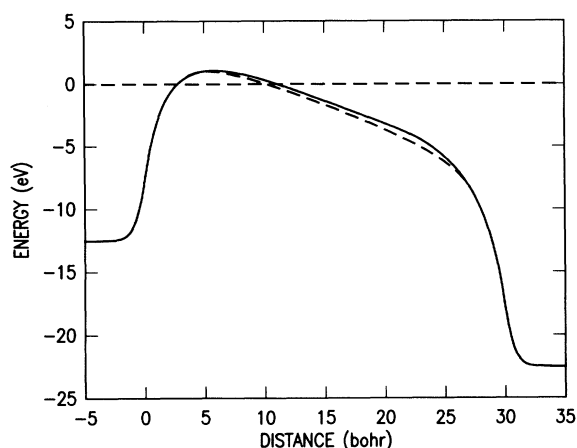


FIG. 4. Surface potential barrier v_{eff} calculated for the jellium model ($r_s = 2$ bohrs) of a bimetallic junction using the local-density approximation for exchange and correlation (solid curve), for 10-V bias. (This bias gives $E = 1.3$ V/Å when the Na atom is present.) Positive-background edges are at 0 and 30 bohrs. The dashed curve shows the effect of replacing the local-density exchange-correlation potential between electrodes with an image potential that saturates near surfaces—the effect is not large.

ing) hornlike structures was recently treated by Glazman *et al.*¹⁰ in the context of the conductance of a constriction. For simplicity, we start with the case of a constant potential floor in the horn. Imagine a ballistic (disorder-free) two-dimensional electronic waveguide, confining the electrons to the region $|y| \leq d(z)$, yielding a “horn” that is smooth on the scale of the electron wavelength $\lambda = 2\pi/k$. This is obtained by taking $d(z)$ to be a function connecting smoothly to the metal electrode at $z = z_-$ where $d(z) = d_-$, having a minimum d_0 at z_0 , and opening into the interelectrode space at z_+ where $d(z) = d_+$. One now makes a Born-Oppenheimer-type separation of the “slow” longitudinal variable z and the “fast” one y . The y problem is just a hard-wall square well having energies $\epsilon_n(z) = (\hbar^2/2m)[n\pi/2d(z)]^2$. As is familiar from the usual separation, $\epsilon_n(z)$ plays the role of an additional potential for the mode n . The adiabatic separation of variables can be used also for more general potentials. So long as the changes in these potentials are smooth enough, we can still consider $\epsilon_n(z)$ to be an (n -dependent) potential for the effectively one-dimensional motion in the z direction, for the n th transverse mode.

An important aspect of the adiabatic picture is that for a wave moving adiabatically along a guide, the mode number n is conserved. An electron in mode n , whose energy is above $\epsilon_n(z_0)$, has a unit probability of arriving at the right, where $d = d_+$, in the same mode, with no scattering into different modes. Since $\epsilon_n(z_0)$ increases with n , the constriction will selectively transmit only those modes with $n \leq n_0$, where n_0 is the maximum n for which $\epsilon_n(z_0) < \epsilon_F$.

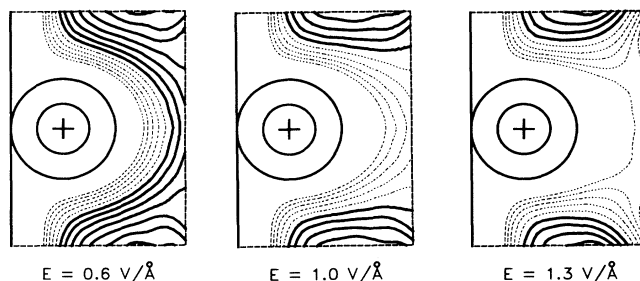


FIG. 5. Contour maps of v_{eff} within the region defined by the dashed rectangle in Fig. 3, for three values of E . The solid contour closest to the atom in each case is that for $v_{\text{eff}} = \epsilon_{\text{F}}^{\text{HP}}$; contours shown for other energy values are spaced by $\frac{1}{4}$ eV, starting at $\epsilon_{\text{F}}^{\text{HP}}$. Contours for values greater than or equal to $\epsilon_{\text{F}}^{\text{HP}}$ are solid; those for values below $\epsilon_{\text{F}}^{\text{HP}}$ are dotted. The saddle point is within the box for $E = 1.3$ V/Å.

Let us consider a horn which opens adiabatically up to z_+ and then radiates into free space.¹¹⁻¹³ If one places a screen far away from the confined region (at a distance L), the probability density one would measure will have the form of the diffraction pattern of a wave emitted from a slit of width $2d_+$. The resulting wave on the screen for mode n will be given by a convolution of the diffraction pattern of a slit of width $2d_+$ with two δ functions at $y = \pm n\pi L/2d_+ + k_z$. Thus the probability density on the screen will have two humps located at these values of y , each of a width of order $\pi L/d_+ + k_z$. Note that for $n = 1$ these two humps will overlap and only a single hump will be seen. The total angular spread due to the diffraction of an electron from channel n is therefore of order θ_n , where

$$\tan \theta_n = (n+1) \frac{\pi}{d_+ + k_z} \sim \frac{2(n+1)}{n_{\text{max}}}, \quad (2)$$

with n_{max} the number of transverse states such that $\epsilon_n(z_+) \leq \epsilon_F$. For the real case, where the potential decreases between the end of the channel and the screen, this discussion is valid with θ_n being the angle and k the wave number immediately after the horn. For this mechanism to yield good focusing, it is necessary that $n_0 \ll n_{\text{max}}$. It can be seen from Eq. (2) that for $n_0 = n_{\text{max}}$, i.e., when all the possible modes at d_+ are populated, the total beam opening will be large. It was found by Garcia and co-workers¹⁴ (see also Ref. 15) that this is indeed the case. To get a narrow emitted beam, it is necessary to have a selection of the modes so that $n_0 \ll n_{\text{max}}$. Such a selection can be achieved by a pure constriction, by a potential barrier in the channel, or by a combination of both.

Consider the potential configuration formed at the tip (Fig. 5). It can be seen that for a large range of field, the potential must have a saddle point. Now consider, e.g., the right-hand map in Fig. 5. At the saddle point, the depth of the confining potential well is minimal.

Therefore, the wave function at this point substantially penetrates the forbidden region and has a rather large extension in transverse directions. For a very shallow well at this point, the transverse momentum of this state will be very small. If the changes in the potential are smooth, the height of the saddle point together with the shape of the well there determine the number of occupied channels that will be transmitted by the constriction. For example, for the right-hand map of Fig. 5, we estimate that only $n=1$ can be transmitted. Approximating the transverse potential at the point of exit from the horn by a parabola, the $n=1$ state would produce a Gaussian beam whose width is given by $\tan\theta_1 \sim (ky_0)^{-1}$, instead of Eq. (2), where y_0 is the distance between the classical turning points for the ground state. (For the right-hand map of Fig. 5, $y_0 \sim 10 \text{ bohr}^{-1}$.)

We have done a calculation for the case in which the constriction in the right-hand map of Fig. 5 was deepened (to a uniform value equal to that of the bottom of the tip-electrode conduction band). The saddle-point structure was thus removed, and the beam then showed a spread of over 70° (as noted earlier). Garcia and co-workers¹⁴ have shown that channel selection can be obtained by tunneling through a potential barrier located past the constriction. Our adiabatic selection mechanism achieves this channel filtering while retaining large transmission probabilities and effective conductances of order $e^2/\pi\hbar [(12900 \Omega)^{-1}]$ per channel for fields $\gtrsim 1 \text{ V/\AA}$. We believe that this mechanism is the one mainly responsible for a beam that is both focused and can carry a large current.

We would like to thank H. Rohrer, R. J. Hamers, M. Büttiker, J. J. Saenz, J. Tersoff, D. A. Smith, R. Gomer, Y. Yacoby, A. R. Williams, and especially H.-W. Fink and N. Garcia, for a number of helpful discussions. Research at the Weizmann Institute was partially supported by grants from the Israeli Academy of Sciences and from the Minerva Foundation, Munich, West Germany.

¹H.-W. Fink, Phys. Scr. **38**, 260 (1988).

²See, in particular, N. D. Lang, Phys. Rev. B **36**, 8173 (1987); Comments Condens. Matter Phys. **14**, 253 (1989).

³The distances between the field-emission tip and a perforated carbon foil in the recent experiments of W. Stocker, H.-W. Fink, and R. Morin (to be published) are much smaller, however.

⁴A. McCann and J. S. Brown, Surf. Sci. **194**, 44 (1988); see also L. Orosz and E. Balázs, Surf. Sci. **177**, 444 (1986).

⁵N. D. Lang and A. R. Williams, Phys. Rev. B **18**, 616 (1978).

⁶Compare the classical treatment of field outside a hemisphere on a conducting surface by D. J. Rose, J. Appl. Phys. **27**, 215 (1956).

⁷With bias adjusted to keep $E=1 \text{ V/\AA}$, replacing the Na tip atom with K decreases δI by 40%.

⁸As E is decreased below 1 V/\AA , this width decreases only rather slowly, but as E is increased past 1 V/\AA , the width begins to increase rapidly, reaching, e.g., $\sim 650 \text{ meV}$ at $E=1.9 \text{ V/\AA}$.

⁹Another difference, of course, is that the tip atom sits on a large flat surface, whereas at least some of the experimental tips may be better represented by, e.g., a paraboloid. A classical trajectory calculation following Ref. 6 for the two tip models of a hemisphere on a plane and a paraboloid with the same radius of curvature shows that for tip-screen distances similar to those used here, the beam spread for the hemisphere is $\sim 20\%$ smaller than for the paraboloid.

¹⁰L. I. Glazman, G. B. Lesovik, D. E. Khmel'nitskii, and R. I. Shekhter, Pis'ma Zh. Eksp. Teor. Fiz. **48**, 218 (1988) [Sov. Phys. JETP Lett. **48**, 238 (1988)].

¹¹A. Yacoby and Y. Imry (to be published).

¹²A. Szafer and A. D. Stone, Phys. Rev. Lett. **62**, 300 (1989).

¹³For a horn with a constant potential, the condition for rays to be controlled by the horn is $d'(z) < \pi n [dk_z]^{-1} = 2n/n_{\max}(d)$. With increasing d' and d , this condition will cease to be satisfied at a point at which the radiation can be thought of as going into free space. This equation places stringent conditions on the flaring of the horn required to get focusing.

¹⁴L. Escapa and N. Garcia, J. Phys. Condens. Matter **1**, 2125 (1989); N. Garcia, J. J. Saenz, and H. De Raedt (to be published). Note also that a version of the potential discussed here was found and analyzed for a macroscopic tip with no atomic structure by P. A. Serena, L. Escapa, J. J. Saenz, N. Garcia, and H. Rohrer, J. Microsc. **152**, 43 (1988).

¹⁵D. van der Marel and E. G. Haanappel, Phys. Rev. B **39**, 7811 (1989).